Flavonoids as Visible Light Photoinitiators

Subjects: Polymer Science

Contributor: Fréderic Dumur

The design of biosourced and/or bioinspired photoinitiators is an active research field as it offers a unique opportunity to develop photoinitiating systems exhibiting better biocompatibility as well as reduced toxicity. In this field, flavonoids can be found in numerous fruits and vegetables so these structures can be of interest for developing, in the future, polymerization processes, offering a reduced environmental impact but also better biocompatibility of the polymers.

photoinitiator visible light photopolymerization

1. Flavonols

Flavonols have been extensively studied in health sciences, due to their low toxicities but also due to their antioxidant and anticancer activities [1][2][3][4][5][6][7][8][9]. Flavonols also possess excellent optical properties [10][11][12][13][14]. Due to the presence of the hydroxy group close to the ketone group, these dyes also exhibit excited state intramolecular proton transfer (ESIPT) properties, enabling these dyes to have large Stokes shifts and a dual emission associated with the formation of two excited states, the first one corresponding to the Franck–Condon excited state and the second one attributed to the tautomeric form issued from ESIPT [15][16][17][18][19][20][21][22][23][24][25][26][27]. Despite these appealing features, several drawbacks can be cited, especially regarding the stability of flavonols under light irradiation. In addition to the aforementioned intramolecular proton transfer [15][16][17][18][28][29][30][31][32][33], photooxidation [34][35][36], reverse proton transfer [37] or photorearrangement reaction [38][39] can be cited as the main photoinduced chemical reactions. Despite this attested instability under irradiation, flavonols were used in photopolymerization. Notably, the remarkable fluorescence of a flavonol derivative was used for the real-time monitoring of the FRP of an acrylate-based E-Shell 300 biocompatible polymer by using the flavanol derivative as a fluorescent probe. However, this flavonol derivative was not used as a photoinitiator/photosensitizer but only as a probe [27].

The first report mentioning the use of flavonoids as photoinitiators of polymerization was reported in 2013 by Lalevée and coworkers [40]. In order to provide sufficient absorption in the visible range, different chromophores were connected to the flavonol scaffold, namely pyrene, anthracene or a *para*-dimethylaminophenyl group (see **Figure 1**).

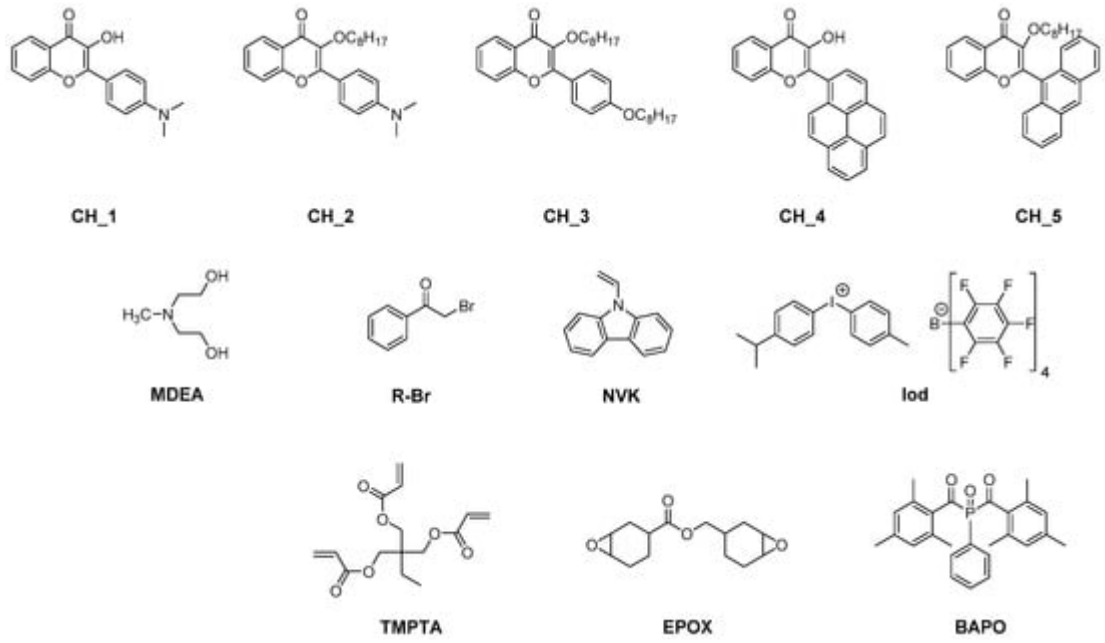

Figure 1. Chemical structures of flavonols CH_1-CH_5, different monomers and additives.

From the absorption viewpoint, modification of the side groups strongly impacted the absorption properties of the dyes. All dyes exhibited an absorption maximum located in the near-UV-visible range, except for CH_4 for which an absorption maximum located at 431 nm was determined in acetone. In the case of CH_1-CH_3 and CH_5, maxima located at 394, 377, 325 and 385 nm were respectively measured in acetonitrile. Noticeably, alkylation of the phenolic group in CH_1 blueshifted the absorption of CH_2 by ca. 17 nm, from 394 nm for CH_1 up to 377 nm for CH_2. Improvement in the electron-donating ability of the side group contributed to the redshift of the absorption, as exemplified with CH_2 exhibiting an absorption redshifted by ca. 50 nm compared to CH_3 bearing a weak electron donor. Considering that the absorption of all dyes extends until the visible range, these dyes were thus appropriate candidates for polymerization experiments performed at 457 nm with a laser diode (I = 100 mW/cm^2), at 462 nm with an LED (I = 15 mW/cm^2) and upon irradiation with a halogen lamp (370–800 nm range, I = 12 mW/cm^2). Two different mechanisms were investigated, an oxidative and a reductive pathway. Among the two possible mechanisms, the oxidative pathway proved to be the most reactive one. By using the three-component dye/Iod/NVK systems (where Iod and NVK respectively stand for [methyl-4-phenyl-(methyl-1-ethyl)-4-phenyl]iodonium tetrakis(pentafluorophenyl)borate and *N*-vinylcarbazole), the phenyl radicals formed by photoinduced electron transfer from the excited dye toward the electron-deficient iodonium salt can further react with NVK, producing Ph-NVK$^\bullet$. These radicals can also react with Iod, generating Ph-NVK$^+$ [41][42][43]. Therefore, this mechanism can contribute to promoting both the free radical polymerization (FRP) of acrylates and the free-radical-promoted cationic polymerization (FRPCP) of epoxides (see Equations (r1)–(r3)). By UV-visible absorption spectroscopy, the formation of CH_1$^{\bullet+}$ could be detected at ca. 500 nm, supporting the oxidation step. The formation of CH_1$^{\bullet+}$ and Ph$^\bullet$ was also evidenced by electron spin resonance (ESR).

$$CH \rightarrow {}^1CH\ (h\nu) {}^1CH + Ph_2I^+ \rightarrow CH^{\bullet+} + Ph_2I^\bullet \text{ and } Ph_2I^\bullet \rightarrow Ph^\bullet + Ph\text{-}I \quad (r1)$$

$$Ph^\bullet + NVK \rightarrow Ph\text{-}NVK^\bullet \quad (r2)$$

$$\text{Ph-NVK}^{\bullet} + \text{Ph}_2\text{I}^{+} \rightarrow \text{Ph-NVK}^{+} + \text{Ph-I} + \text{Ph}^{\bullet} \text{(r3)}$$

In the case of the three-component dye/MDEA/R-Br system (where MDEA and R-Br stand for *N*-methyldiethanolamine and phenacyl bromide), the formation of phenacyl radicals could be identified as the unique radicals formed with this three-component system during the ESR experiments (see Equations (r4) and (r5)).

$$^{1}\text{CH} + \text{MDEA} \rightarrow \text{CH}^{\bullet -} + \text{MDEA}^{\bullet +} \text{(r4)}$$

$$\text{CH}^{\bullet -} + \text{R-Br} \rightarrow \text{CH} + \text{R}^{\bullet} + \text{Br}^{-} \text{(r5)}$$

Examination of the photoinitiating abilities of CH_1–CH_5 during the CP of (3,4-epoxycyclohexane)methyl 3,4-epoxycyclohexylcarboxylate (EPOX) upon irradiation with a halogen lamp revealed CH_1 to outperform the other dyes. Thus, a conversion of 60% after 800 s of irradiation was determined, contrarily to 30–40% for CH_2-CH_5 in the same conditions. Using CH_1 as the chromophore, a slightly higher EPOX conversion was determined at 457 nm (65% conversion vs. 60% with the halogen lamp).

Comparison with the reference three-component phenyl*bis*(2,4,6-trimethylbenzoyl)phosphine oxide (BAPO)/Iod/NVK system revealed CH_1 to furnish similar monomer conversions to BAPO in three-component systems. While examining the FRP of trimethylolpropane triacrylate (TMPTA) using the reductive pathway, only CH_1 and CH_2 could furnish acceptable monomer conversions. If no monomer conversion could be detected with the two-component CH_1 or CH_2/MDEA systems, a conversion of ca. 40 and 35% could be obtained after 300 s of irradiation with a halogen lamp using the three-component CH_1/MDEA/R-Br (0.5%/4%/3% *w*/*w*) and CH_2/MDEA/R-Br (0.5%/4%/3% *w*/*w*) systems. This conversion could be significantly increased by using a laser diode emitting at 457 nm. In these conditions, a conversion of 60% could be determined using the three-component CH_1/MDEA/R-Br (0.5%/4%/3% *w*/*w*) system. Comparison with the reference two-component Eosin-Y/MDEA (0.1%/3% *w*/*w*) system (30% conversion after 300 s) revealed the two three-component systems based on CH_1 and CH_2 to outperform the reference system. Considering that cations and radicals are both formed with the three-component CH_1/Iod/NVK system, the elaboration of interpenetrated polymer networks by the concomitant polymerization of TMPTA and EPOX was examined under air. After 1000 s of irradiation at 457 nm with a laser diode, photopolymerization of a TMPTA/EPOX blend (50%/50%) under air furnished tack-free polymers. Using low light intensities (LED@462 nm and a halogen lamp), 30 min. was required to get tack-free coatings.

In 2016, the first natural flavonoid dye, namely quercetin (3,5,7,3′,4′-pentahydroxyflavone), was examined by Versace and coworkers both as a photosensitizer and an antibacterial agent for the design of antibacterial coatings [44]. Indeed, an efficient strategy to cause the apoptosis of bacteria consists in producing reactive oxygen species (ROS) that will be capable of degrading cells [45][46][47][48]. Among ROS, singlet oxygen constitutes the best approach to prevent microorganism adhesion and proliferation on any surface. Several photoinitiators of polymerization have been identified as providing antimicrobial properties to coatings such as hydroxyethyl Michler's ketone [49], rose Bengal [50][51], porphyrins and phthalocyanines [52][53], eosin Y [50][54], toluidine blue [55] or

methylene blue [55][56][57]. If these synthetic dyes showed interesting properties, a step further consists in using natural dyes to act as antibacterial agents, which constitutes a major environmental challenge.

Quercetin also exhibits antiviral, anti-inflammatory, anti-allergic and antioxidant activities, and this natural compound is also beneficial to limit cancer risks and cardiovascular problems [58][59][60]. Considering that quercetin is responsible for the green color of oak leaves, an absorption extending up to 430 nm was determined in acetonitrile, with an absorption maximum at 370 nm (ε = 19,000 $M^{-1}{\cdot}cm^{-1}$). An emission peak was also determined at 535 nm so that a Stokes shift of 8350 cm^{-1} could be calculated. This large Stoke shift is indicative of a significant electronic change between the ground state and the excited state. Photolysis experiments performed with the two-component quercetin/Iod1 system revealed the photogeneration of Bronsted acid (H^+) using rhodamine B as an acid indicator. Quercetin was thus identified as a promising candidate for CP.

Using glycerol triglycidyl ether (GTE) as the monomer and upon irradiation with a Xe lamp (I = 70 mW/cm^2), a GTE conversion of 75% could be determined after 1200 s of irradiation using the two-component quercetin/Iod1 (2.5%/4% *w*/*w*) system (where Iod1 stands for 4-(2-methylpropyl)phenyl iodonium hexafluorophosphate). Interestingly, the quercetin-based coatings exhibited remarkable thermal stability since a decomposition temperature higher than 375 °C could be determined by thermogravimetric analysis (TGA). Examination of the fluorescence of the polymer films revealed the presence of remaining quercetin that could be advantageously used to generate reactive oxygen species upon light activation. Antibacterial properties were examined with Gram-negative bacteria (*E. coli*) and Gram-positive bacteria (*S. aureus*). Noticeably, quercetin-based coatings only exhibited antiproliferation properties for Gram-positive bacteria. In the case of *E. coli*, the development of bacteria was neither inhibited by light nor affected by the presence of quercetin within the polymer film. On the contrary, a total death of Gram-positive bacteria (*S. aureus*) was determined after 2 h of irradiation. The insensitivity of Gram-negative bacteria to singlet oxygen was assigned to the presence of lipopolysaccharides in the cell wall offering some protection against exogenous agents.

More recently, quercitin and morin, which are two isomers of position, were compared for their photoinitiating abilities during the FRP of a BisGMA/TEGDMA (1/1) blend (where BisGMA and TEGDMA stand for bisphenol A-glycidyl methacrylate and triethylene glycol dimethacrylate, respectively) or TMPTA, the cationic polymerization of tri(ethylene glycol) divinyl ether (DVE-3), and the polymerization thiol-ene of a DVE-3/trimethylolpropane *tris*(3-mercaptopropionate) (Trithiol) (1/1) blend or a 1,3,5-triallyl-1,3,5-triazine-2,4,6(1*H*,3*H*,5*H*)-trione (Trione)/Trithiol (1/1) blend (see **Figure 2**) [61]. Morin is a natural compound that can be extracted from Osage orange and is well known to exert antioxidant, anti-inflammatory and anti-carcinogenic effects [62][63][64][65].

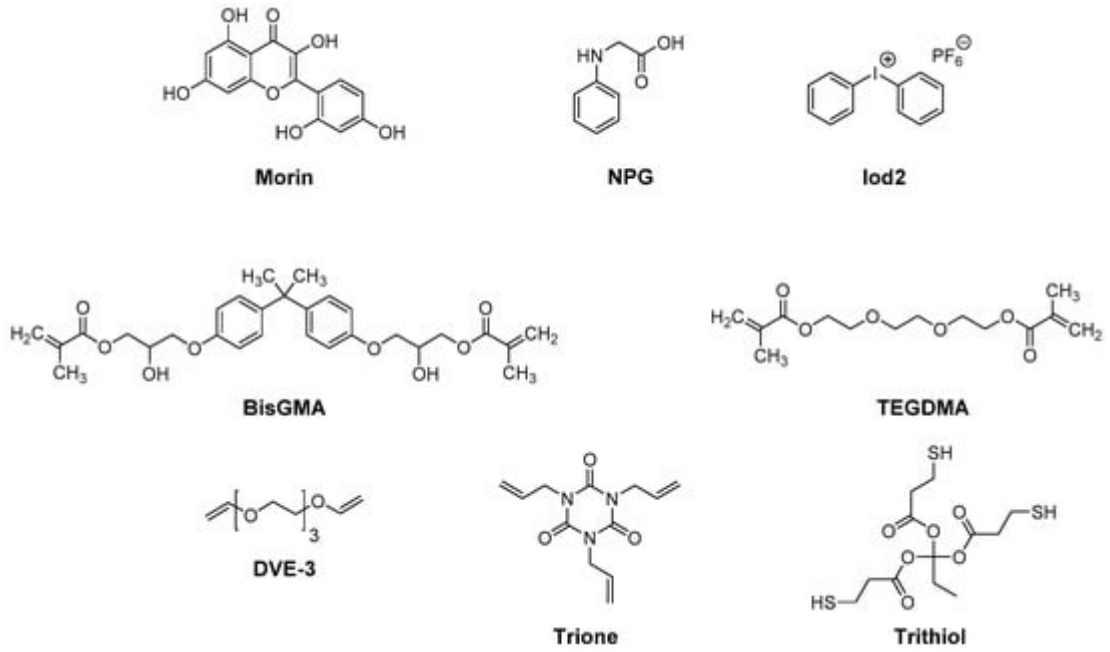

Figure 2. Chemical structure of quercetin and its isomer of position morin, different monomers and additives.

From the absorption viewpoint and despite the similarity of structures between quercetin and morin, totally different absorption spectra were determined in ethanol. If no absorption peaks could be detected for morin, an absorption peak could be clearly detected for quercetin (λ_{max} = 372 nm, ε = 23,300 $M^{-1}{\cdot}cm^{-1}$). In addition, the absorption spectrum of morin extends up to 575 nm so that polymerization experiments could be carried out at 374, 394, 410 and 445 nm.

FRP experiments performed with morin and quercetin revealed the two-component morin/Iod2 system to be unable to initiate the FRP of the BisGMA/TEGDMA (70/30 *w*/*w*) blend upon irradiation at 410 and 445 nm. Conversely, a conversion of 26% was obtained with the quercetin/Iod2 system upon excitation at 410 nm (I = 110 mW/cm^2) for 300 s. No polymerization was detected at 445 nm with quercetin due to the lack of absorption. A significant improvement in the monomer conversion was obtained by using the three-component quercetin/Iod2/*N*-phenylglycine (NPG) (0.5%/2%/2% *w*/*w*/*w*) system. A conversion of 60% at 410 nm and 57% at 445 nm. These values are higher than those obtained with the reference NPG/Iod2 system (26% at 410 nm, 47% at 445 nm). While examining the cationic polymerization (CP) of DVE-3, the best monomer conversion was obtained at 410 nm with the two-component quercetin/Iod2 (0.5%/2% *w*/*w*) system (89% after 300 s of irradiation) vs. 78% with the morin/Iod2 system. Parallel to this, an induction time of 25 s was determined with the quercetin-based system contrarily to 110 s with morin. Finally, the two-component quercetin/Iod2 (0.5%/2%, *w*/*w*) system was examined for the thiol-ene polymerization of the DVE-3/Trithiol (1/1) and Trione/Trithiol (1/1) blends.

Interestingly, DVE-3 was entirely polymerized in the presence of Trithiol for which a trithiol conversion of only 51% was detected. A shorter induction time was determined for DVE-3, reduced to only 8 s contrarily to 25 s for the homopolymerization of DVE-3. By replacing DVE-3 with Trione, a similar conversion was obtained for Trione and Trithiol, around 80% for the two monomers. To support the unequal monomer conversion determined during the

thiol-ene polymerization of a DVE-3/Trithiol blend, the occurrence of a homopolymerization of DVE-3 concomitant to the thiol-ene polymerization was suggested. Conversely, homopolymerization of Trione is difficult, avoiding this undesired reaction [66][67][68].

In 2018, another flavonol, i.e., 3-hydroxyflavone (3HF) was used in combination with an amino acid, namely *N*-phenylglycine (NPG), to produce free radicals upon irradiation at 385, 405 and 477 nm (see **Figure 3**) [69].

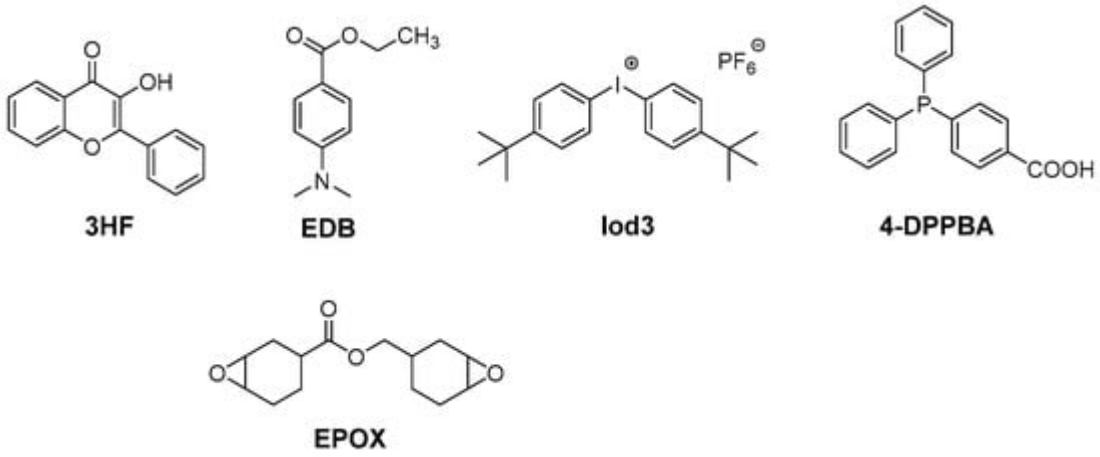

Figure 3. Chemical structures of 3HF, different monomers and additives.

From the absorption viewpoint, the absorption maximum of 3HF was blue-shifted by ca. 20 nm compared to quercetin (350 nm vs. 370 nm for 3HF). Only low molar extinction coefficients could be determined in the visible range, ranging between ε ~ 250 $M^{-1}{\cdot}cm^{-1}$ at 405 nm and ε ~ 40 $M^{-1}{\cdot}cm^{-1}$ at 470 nm. Conversely, at 350 nm, a molar extinction coefficient of ε~14,000 $M^{-1}{\cdot}cm^{-1}$ could be calculated. The high reactivity of 3HF was evidenced when combined with NPG. Thus, using the 3HF/NPG (0.5%/1% *w*/*w*) couple, a conversion as high as 71% could be determined during the FRP of a BisGMA/TEGDMA (1/1) blend (where BisGMA and TEGDMA stand for bisphenol A-glycidyl methacrylate and triethylene glycol dimethacrylate, respectively) upon irradiation at 405 nm with an LED (I = 110 mW/cm^2).

This value is higher than that obtained with the reference Iod3/EDB (1%/1% *w*/*w*) system (68% after 100 s of irradiation at 405 nm) [70]. If an excellent monomer conversion could be obtained with the reductive pathway, a different situation was found using the oxidative one. Thus, only a low monomer conversion of 19% was obtained with the two-component 3HF/Iod3 (0.5%/1% *w*/*w*) system upon irradiation at 405 nm. By using the three-component 3HF/Iod3/NPG (0.5%/1%/1% *w*/*w*/*w*) system, high monomer conversions could be determined at 405 and 477 nm (79 and 65%, respectively). In particular, the monomer conversion of 65% obtained at 477 nm is remarkable, considering the weak molar extinction coefficient of 3HF at 477 nm. The crucial role of the amine in the monomer conversion was evidenced by replacing NPG with ethyl 4-(dimethylamino)benzoate (EDB). In this case, the conversion was reduced to only 17%. The difference in reactivity for the three-component system based on EDB and NPG can be ascribed to the decarboxylation reaction occurring with NPG, avoiding back electron transfer [71][72]. Upon irradiation at 385 nm, the CP of EPOX furnished the high conversion of 55% after 100 s of irradiation with the three-component 3HF/Iod3/EDB (0.5%/1%/1% *w*/*w*/*w*) system. For comparison, only an EPOX conversion

of 15% was obtained with the reference BAPO/Iod3 (0.5%/1% *w*/*w*) system in the same conditions. Considering the high performance of the different photoinitiating systems designed with 3HF as a photosensitizer, interest in these photoinitiating systems was demonstrated during direct laser writing experiments and during the design of composites. In the case of the direct laser writing experiments, 3D patterns exhibiting an excellent spatial resolution could be evidenced.

Composites were obtained by impregnating a BisGMA/TEGDMA (70%/30%) resin with glass fibers (50% glass fiber/50% resin). Using the 3HF/NPG combination, composites could be fully cured in only one pass (2 m/min belt speed) upon irradiation with an LED emitting at 395 nm.

To support the high efficiency of the 3HF/NPG and 3HF/Iod3 systems, the following mechanisms could be determined by combining steady-state photolysis and fluorescence quenching experiments, ESR and electrochemistry (see Equations (r6)–(r12)).

$$3HF \rightarrow {}^{1,3}3HF\ (h\nu) \text{(r6)}$$

$${}^{1,3}3HF + NPG \rightarrow (3HF\text{-}H)^{\bullet} + NPG_{(-H)}{}^{\bullet} \text{(r7)}$$

$$NPG_{(-H)}{}^{\bullet} \rightarrow NPG_{(-H;-CO2)}{}^{\bullet} \text{(r8)}$$

$${}^{1,3}3HF + Iod \rightarrow 3HF^{\bullet+} + Ar_2I^{\bullet} \rightarrow Ar^{\bullet} \text{(r9)}$$

$$NPG + Iod \leftrightarrow [NPG\text{-}\ Iod]_{CTC} \text{(r10)}$$

$$[NPG\text{-}\ Iod]_{CTC} \rightarrow \rightarrow \rightarrow Ar^{\bullet}\ (h\nu) \text{(r11)}$$

$$NPG_{(-H;-CO2)}{}^{\bullet} + Ar_2I^{+} \rightarrow NPG_{(-H;-CO2)}{}^{+} + Ar^{\bullet} + ArI \text{(r12)}$$

In 2020, 3HF was revisited by Wang and coworkers in a series of seven flavonols differing in the substitution pattern (see **Figure 4**) [73]. The influence of halogens on the photoinitiating ability of flavonols could be examined, these groups being introduced at different positions on the flavonol core.

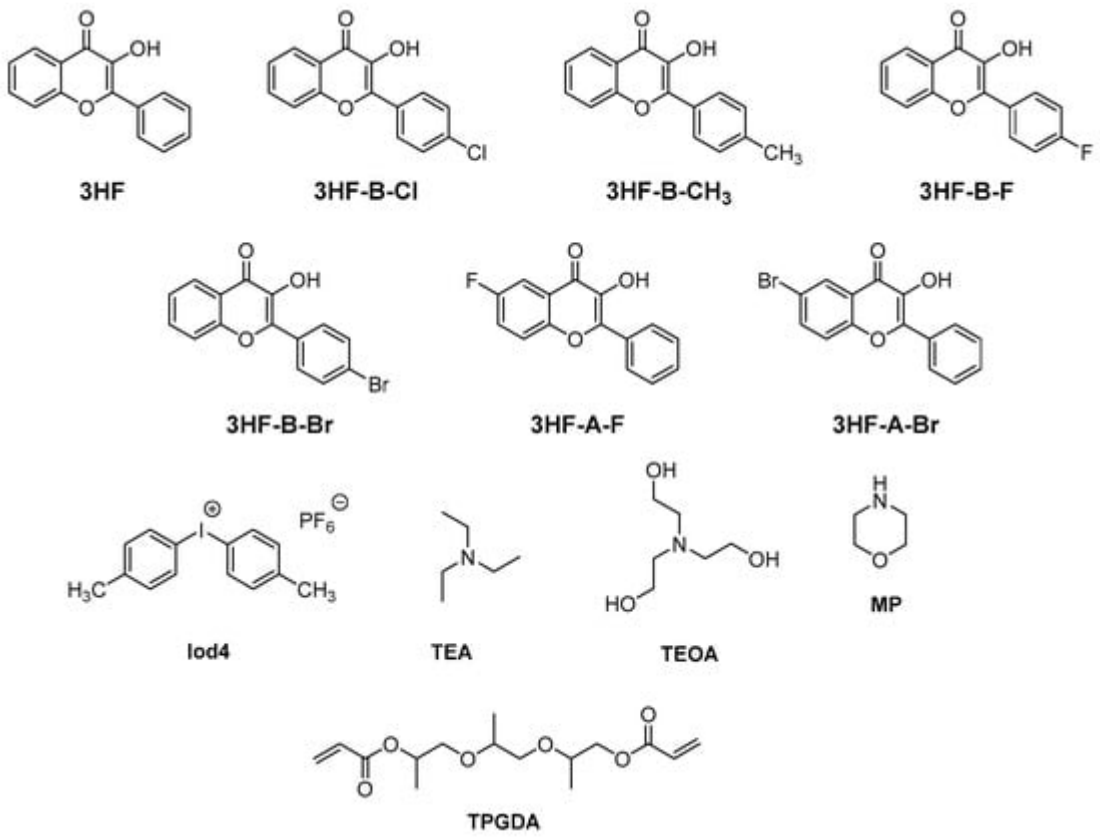

Figure 4. Chemical structures of different derivatives of 3HF, the monomer and different additives.

Noticeably, the absorption of the different dyes was not significantly affected by the halogen substitution, and absorption in the 280–450 nm range could be determined for all dyes. Thus, absorption maxima between 342 nm for 3HF and 3HF-B-F and 349 nm for 3HF-A-F were determined in methanol. Examination of the fluorescence properties of the different 3HF revealed the presence of two emission peaks, the first one at ca. 450 nm, corresponding to the Franck–Condon excited state, and the second one at 550 nm, corresponding to the emission of the tautomer formed by ESIPT. In the case of 3HF-A-F and 3HF-A-Br, emission peaks at 450 nm could not be detected for these tow dyes, attributable to a fast ESIPT process.

Based on their absorption spectra, photopolymerization experiments were carried out at 385 nm. Photolysis experiments performed at 385 nm for the two-component dye/triethanolamine (TEOA) and dye/Iod4 systems revealed the photolysis rate to be higher for the two-component dye/Iod4 systems. The different dyes are thus easier to oxidize than to reduce. Fluorescence quenching experiments performed in methanol revealed the fluorescence of the ESIPT tautomer to be drastically reduced by increasing the concentration of Iod4 and TEOA, evidencing the reaction with the additives to be faster than the ESIPT process. In the case of the two-component dye/Iod4 systems, the formation of three different 3HF-based toluene adducts resulting from the addition of the toluene radical (formed by photoinduced electron transfer between the excited dye and the iodonium salt) to the 3HF dyes was detected by mass spectrometry.

Photopolymerization experiments were carried out on a difunctional monomer, namely tripropylene glycol diacrylate (TPGDA). Among the four amines tested for the two-component dye/amine systems (TEOA, morpholine (MP),

triethylamine (TEA) and NPG) and irrespective of the 3HF derivatives examined, the highest monomer conversions were obtained with TEOA, whereas the lowest conversions were determined with NPG. Using TEOA as the amine, the influence of the substitution pattern on the photoinitiating ability could be examined. Thus, it was found that the introduction of halogens on the pendant phenyl ring was favorable for monomer conversions compared to the flavonol core. higher monomer conversions were obtained with 3HF-B-F and 3HF-B-Br compared to their 3HF-A-F and 3HF-A-Br analogs. Except for 3HF-B-CH_3 and 3HF-A-Br, which furnished monomer conversions around 70% after 180 s of irradiation, all the other dyes furnished similar monomer conversions, peaking at 80%. While examining the series of flavonols substituted with different groups on the pendant phenyl ring, the introduction of electron-donating groups (such as 3HF-B-CH_3) reduced the monomer conversion and the polymerization rate, whereas the introduction of electron-withdrawing groups improved both the conversion and the polymerization rates. A different trend was found for the dye/Iod3 system. Using the dye/Iod4 (0.2%/1% *w*/*w*) system, the highest polymerization rate was obtained with 3HF-B-CH_3, followed by 3HF-B-Cl, 3HF-B-Br, 3HF-B-F and 3HF. If different polymerization rates were determined using Iod4 as the co-initiator, similar conversions were obtained after 120 s of irradiation at 385 nm. A comparison with identical halogen atoms revealed the brominated derivatives to be more reactive than the fluorinated ones, and this trend of reactivity is comparable to that determined with the two-component dye/TEOA systems.

In 2021, the same group developed an innovative strategy for the design of photoinitiating systems based on flavonols. Considering that the presence of the OH group is responsible for the ESIPT process which is a competitive process to photoinitiation, this intramolecular proton transfer could be efficiently avoided by etherifying or esterifying the OH group with benzoyl or benzenesulfonyl groups [74]. Using this strategy, the ESIPT process could be suppressed, and the design of highly efficient Type I photoinitiators became possible (see **Figure 5**). In particular, the triplet lifetime could be increased, and a reduction in the fluorescence intensity was jointly observed, resulting in an improvement in the photopolymerization efficiency.

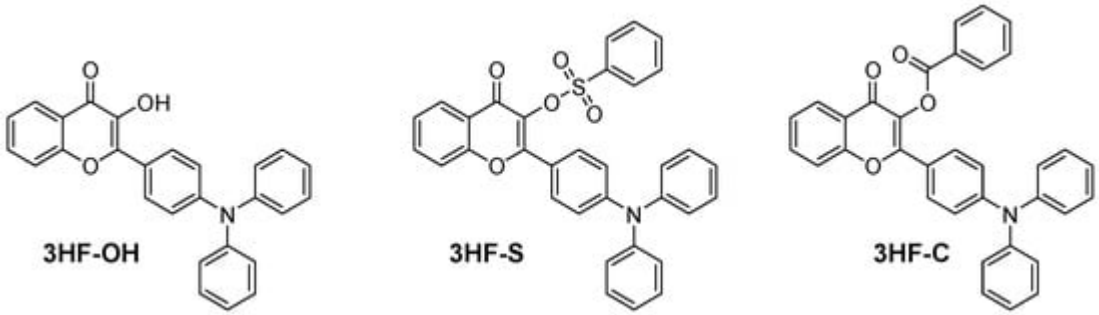

Figure 5. Chemical structures of flavonol-derived Type I photoinitiators.

Noticeably, 3HF-S and 3HF-C could act as efficient monocomponent systems during the FRP of TPGDA but also in combination with TEOA or Iod4 upon irradiation at 405 and at 460 nm with LEDs. Photopolymerization results also revealed the polymerization efficiency of 3HF-S to be higher than that of 3HF-C and 3HF-OH. In particular, the polymerization efficiency of 3HF-S could be greatly improved by decreasing the photoinitiator content, 3HF-S exhibiting aggregation-induced emission (AIE) properties adversely affecting its polymerization efficiency. From the

absorption viewpoint, the presence of the triphenylamine moiety was the key element to redshift the absorption of 3HF-C, 3HF-S and 3HF-OH compared to those previously reported by Lalevée and coworkers [40]. Thus, absorption maxima located at 384, 386 and 396 nm were determined for 3HF-C, 3HF-S and 3HF-OH. Interestingly, the broad absorption band extending up to 480 nm enabled the polymerization tests to be carried out at 405 nm but also at a longer wavelength, namely 460 nm. The solubility of photoinitiators is an important parameter governing the reactivity. Indeed, a low solubility in monomers will adversely affect the polymerization efficiency. 3HF-S exhibited the highest solubility of the three dyes. In particular, compared to 3HF-OH, an improvement in the solubility was determined for the OH-substituted dyes, namely 3HF-C and 3HF-S. Among these dyes, 3HF-S showed the best solubility in aqueous solutions, favorable to polymerization processes used in green conditions. The photoacid generation abilities of 3HF–S and 3HF–C were also examined in acetonitrile using Rhodamine B as an acid indicator upon irradiation with an LED at 405 nm. Interestingly, 3HF-S exhibited the best photoacid generation ability (ϕ_{H+} = 0.2), significantly higher than that of 3HF-C for which a value of only 0.002 was determined. This is directly related to the fact that benzenesulfonic acid is generated with 3HF-S after photocleavage, contrary to benzoic acid in the case of 3HF-C.

FRP experiments of TPGDA performed at 405 and 460 nm revealed the photoinitiating ability of 3HF-C and 3HF-S to outperform that of the reference 3HF-OH. Using 3HF-S as a monocomponent system at 405 nm, a photoinitiator concentration as low as 0.125 wt% could be used while maintaining a high monomer conversion. Eighty-percent conversions could thus be obtained after 180 s of irradiation at 405 nm using 3HF-S. Conversely, no monomer conversion could be detected with 3HF-OH when used as a monocomponent system. The use of 3HF-S in a two-component system enabled drastic shortening of the reaction time using additives such as triethanolamine (TEOA) or triethylamine (TEA) as the amines. By using TEA and TOEA, 80% conversions could be obtained within 20 s. A threefold elongation of the reaction time was determined by using MP and EDB as the amines. Finally, by using NPG as the additive for 3HF-S, 180 s were required to get 80% TPGDA conversion (see **Figure 19**). Comparisons of the TPGDA conversions obtained with camphorquinone (CQ) in one- and two-component systems revealed the 3HF-S-based systems to outperform those prepared with camphorquinone, irrespective of the irradiation wavelength (405 nm or 460 nm). 3HFs were also used for the sensitization of Iod4. In this case, short reaction times (i.e., 20 s) were determined with all systems, evidencing that 3HFs were easier to oxidize than to reduce. Conversions ranging between 85 and 90% could be obtained within 30 s.

Considering the good solubility of 3HF-S in water, the polymerization of hydrogels could be performed at 405 nm. Using PEGDA (70% in water), an excellent monomer conversion could be determined by using a photoinitiator content as low as 0.042 wt%. After 60 s of irradiation at 405 nm, final conversions of 33, 75 and 85% were determined by using 3HF–S (0.042 wt%), 3HF-S/TEOA (0.042%/3% *w*/*w*) and 3HF-S/Iod4 (0.042%/3% *w*/*w*), respectively.

By ESR spin-trapping experiments, the photochemical mechanism involved with the one- and two-component systems could be determined, and the results are summarized in Scheme 1.

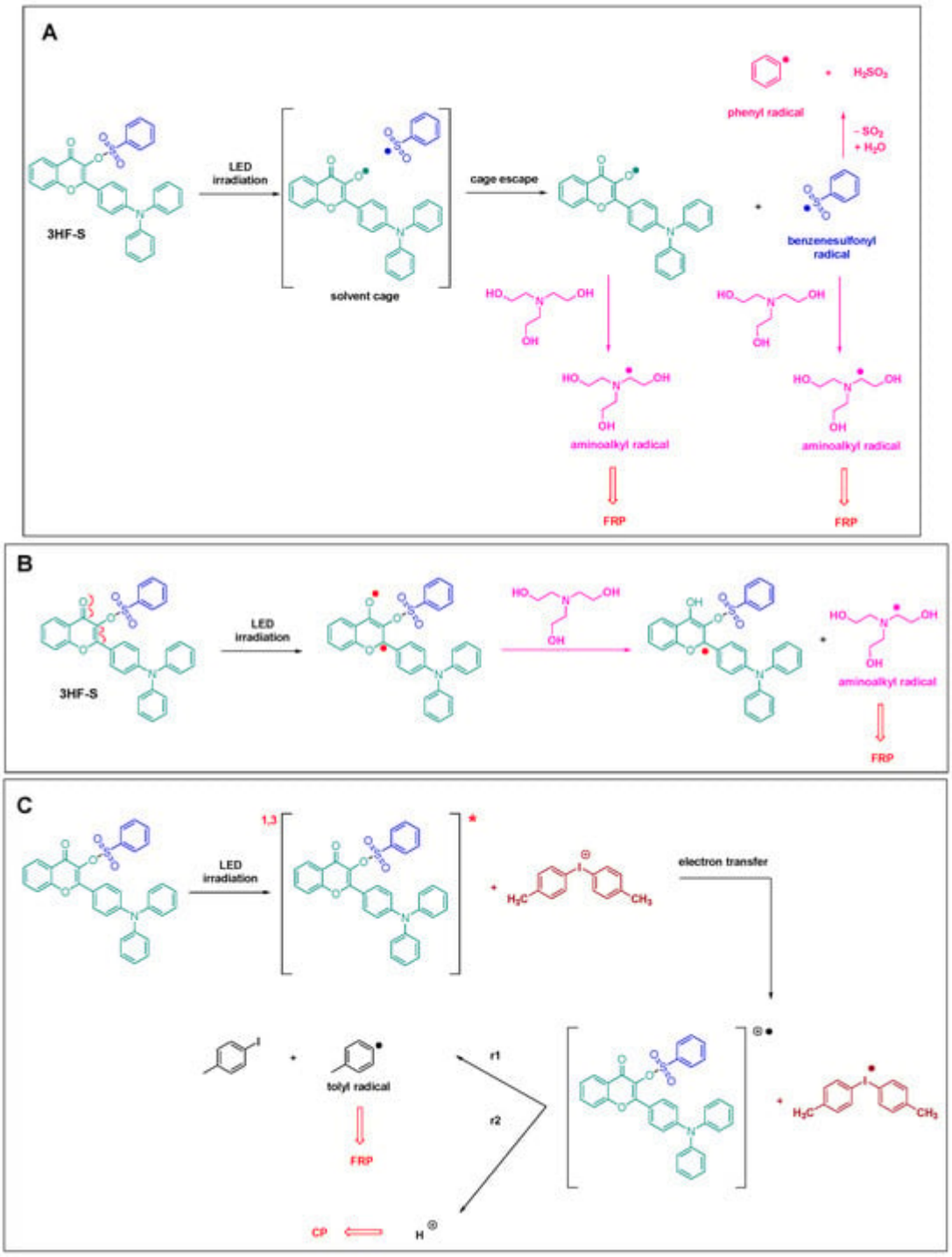

Scheme 1. Photochemical mechanism involved with the different one- and two-component systems (**A**) and (**B**) The two possible mechanism of reaction of 3HF-S with TEOA and (**C**) reaction of 3HF-S with an iodonium salt.

Examination of the cytotoxicity of the polymer films prepared with CQ, 3HF-S and 3HF-C revealed the cell viability of HeLa cells to be higher than 80%, whereas cell viability lower than 80% was determined for polymers prepared with 3HF-OH. Considering that sulfonate derivatives can outperform all other derivatives, another sulfonate derivative, i.e., 3HF-F, was examined, bearing a pendant carbazoyl group [75]. Using this high-performance

photoinitiator in three-component 3HF-F/Iod4/TEOA (0.5%/2%/1% *w*/*w*/*w*) systems, 4D-printed objects could be designed and synthesized.

It has to be noticed that this strategy (hydration/dehydration) has been extensively used by Lalevée and coworkers for designing 4D-printed objects by using chalcones as the chromophores [76][77][78][79].

In 2023, an interesting strategy was developed for the design of Type I photoinitiators, consisting in introducing a camphorquinone derivative on the photocleavable side [80]. Five derivatives were investigated, differing by the substitution of the flavonol core (see **Figure 6**).

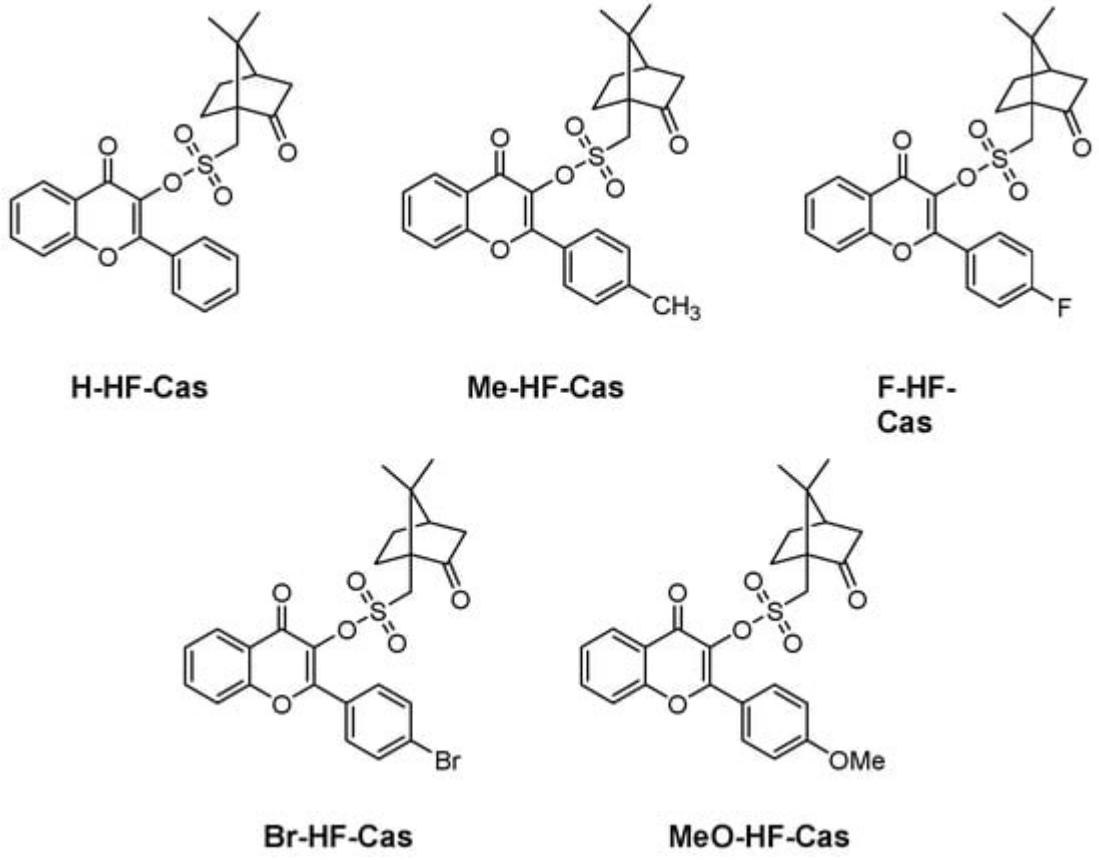

Figure 6. Chemical structures of Type I photoinitiators based on camphorsulfonate.

The choice of camphorsulfonic acid as the additional chromophore was motivated by the different advantages this photoinitiator exhibits such as low sensitivity to oxygen, good water solubility and low toxicity [81][82]. From the absorption viewpoint, almost similar absorption maxima were determined for the different dyes, except for MeO-HF-Cas bearing an electron donating group and for which a redshifted absorption was determined. Thus, absorption maxima located at 294, 295, 296, 300 and 313 nm were respectively determined for H-HF-Cas, F-HF-Cas, Br-HF-Cas, Me-HF-Cas and MeO-HF-Cas.

Examination of their fluorescence properties also revealed that the different dyes exhibit a dual emission, with an emission in the UV range and a second one in the visible range. Even if the ESIPT effect is hindered by the

substitution of the OH group at the C_3-position, the intramolecular charge transfer still exists, with the presence of tautomers in the excited state, as shown in Scheme 2. Considering the similarity of emission around 530 nm, the low contribution of the aromatic ring on the fluorescence de-excitation process was determined.

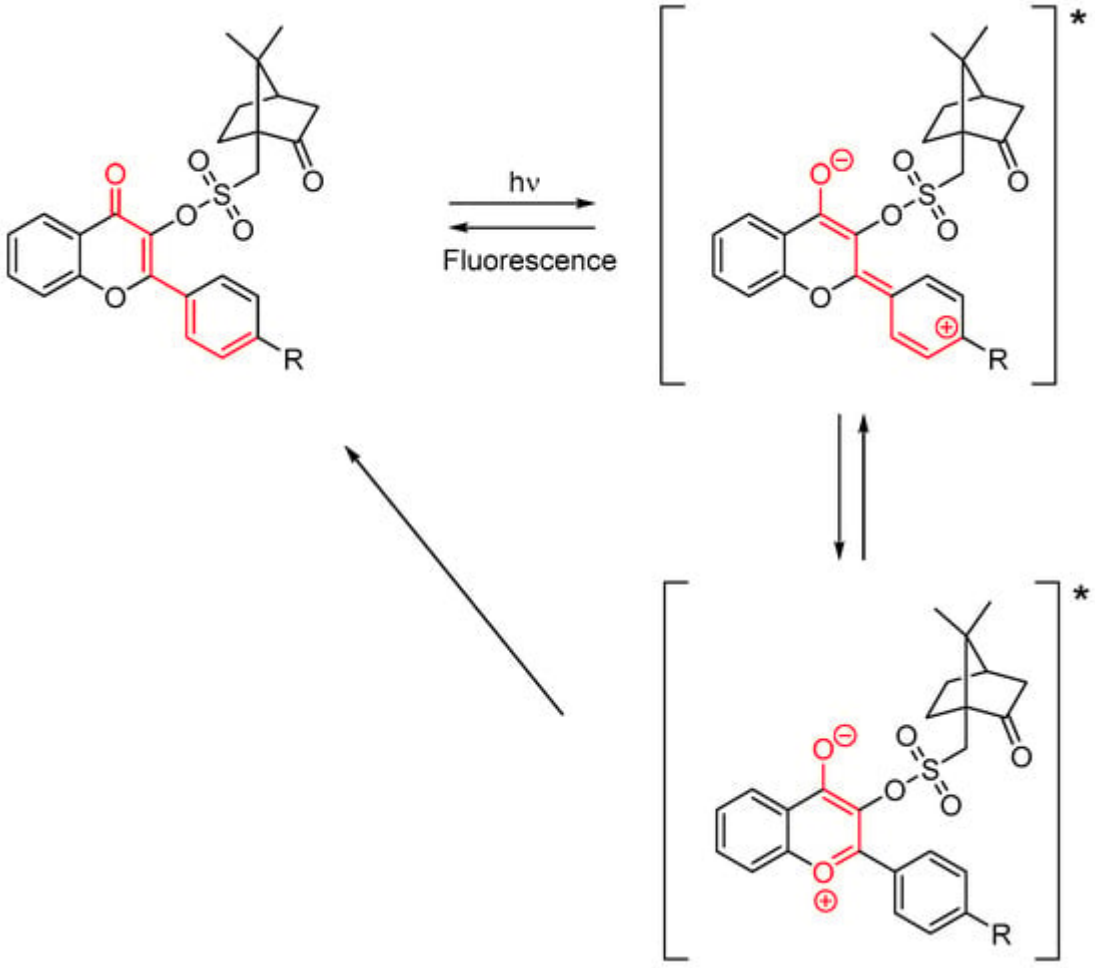

Scheme 2. Rearrangement of flavonol camphorsulfonates in the excited state (*).

Photolysis experiments performed in acetonitrile confirmed the Type I behavior of the different flavonol camphorsulfonates. Upon irradiation at 365 nm, photocleavage of flavonols can clearly be evidenced by NMR. Investigation of the photolysis products by mass spectrometry enabled people to confirm the formation of camphorsulfonic acid and the corresponding flavonol due to water traces in acetonitrile (see Scheme 3). Flavonol camphorsulfonates can thus behave as photoacid generators [83].

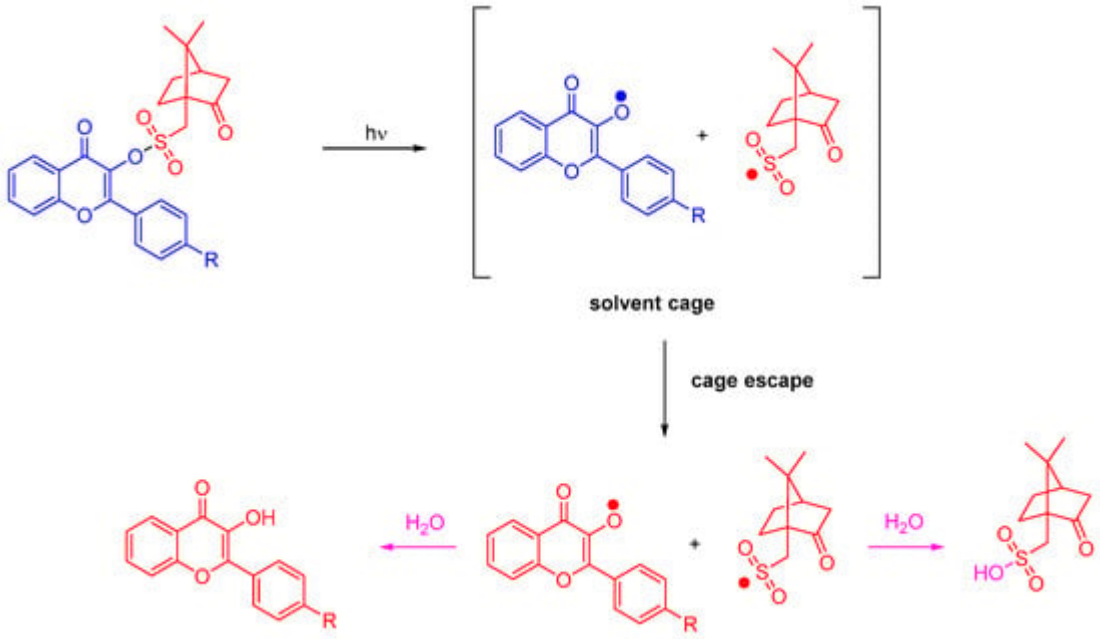

Scheme 3. Mechanism of photolysis of flavonol camphorsulfonates.

The highest photoacid generation quantum yield was determined for Br-HF-Cas bearing a halogen atom upon excitation at 365 nm. In this context, the cationic polymerization of DVE-3 was examined with the different photoinitiators. Upon excitation at 365 nm, only low monomer conversions were obtained using a 1 wt% photoinitiator, consistent with the low photoacid generation ability of camphorsulfonic acid and the inability of the flavonol moiety to initiate a cationic polymerization process. By using flavonol camphorsulfonates as monocomponent systems (1 wt%), the free radical polymerization of PEGDA could be efficiently initiated, and conversions of 80, 96, 91, 88 and 67% were respectively obtained with Me-HF-Cas, F-HF-Cas, Br-HF-Cas, MeO-HF-Cas and H-HF-Cas. By using the different flavonol camphorsulfonates as photosensitizers for Iod4, a slight improvement in the PEGDA conversion could be detected with the two-component dye/Iod4 (0.1%/0.1% *w*/*w*) systems. Thus, PEGDA conversions of 90, 84, 86 and 85% could be obtained after 120 s of irradiation at 365 nm using MeO-HF-Cas, Me-HF-Cas, Br-HF-Cas, F-HF-Cas and Me-HF-Cas.

2. Flavones

Flavonoids are composed of a large group of polyphenolic dyes, and flavone is one of them. Flavone was used as early as 2016 for the photoinduced controlled/“living” polymerization of MMA [84]. Using an LED emitting in the 350–440 nm range, linear PMMA polymers with a polydispersity index (PDI) ranging between 1.34 and 1.42 could be prepared by photopolymerization. Even if the approach is promising, the control of the polymerization process is still lower than what can be currently obtained by thermal polymerization. Photopolymerization is more classically used for the polymerization of multifunctional monomers, and this point was only recently examined by Lalevée and coworkers for the FRP of a dental resin, i.e., a BisGMA/TEGDMA 70/30 blend (see **Figure 7**) [85]. Different flavones were investigated, all these derivatives being natural products. Notably, chrysin can be found in the flowers of blue passionflower (Passiflora caerulea) and myricetin in various edible plants such as onion leaves, Semambu leaves,

bird chili, black tea, papaya shoots and guava [86][87][88][89][90][91][92][93]. As specificities, these dyes are also (poly)phenolic dyes, and phenols are extensively used as stabilizers for monomers [94][95]. In addition, efficient polymerization processes could be performed with these structures.

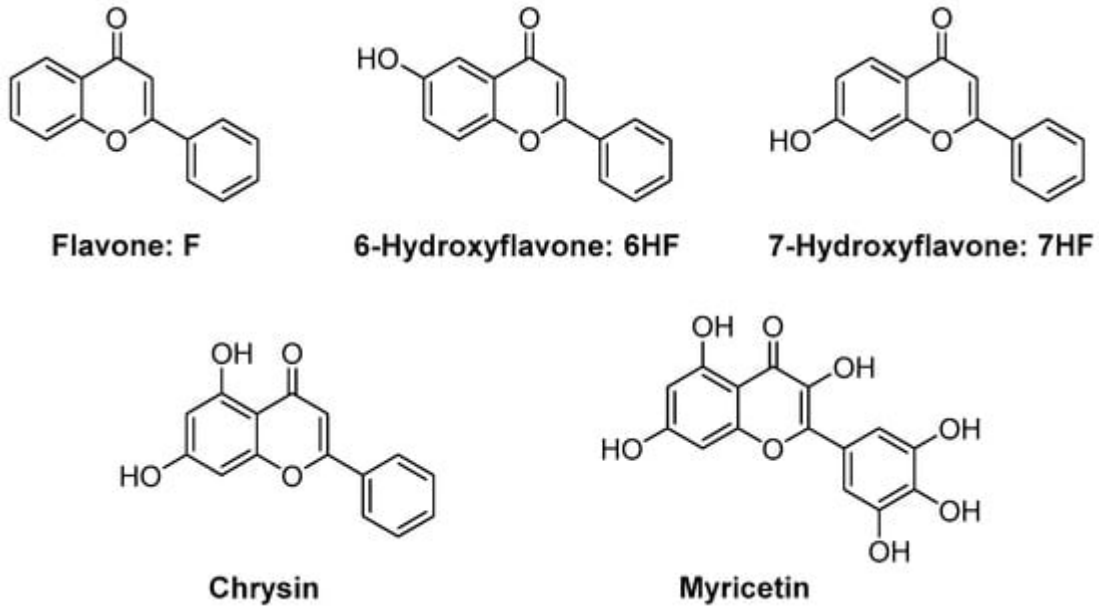

Figure 7. Chemical structures of different flavones used as photoinitiators of polymerization.

all dyes exhibit UV-centered absorption, except for myricetin for which a redshift of the absorption was detected for this dye. It can be assigned to the presence of the numerous OH groups acting as electron-withdrawing groups, improving the electronic delocalization existing in this structure. An absorption extending up to 450 nm could be determined for Myricetin, whereas almost no absorption could be detected anymore for the other dyes. The efficiency of the polymerization process is also strongly related to the solubility of the photosensitizers in resins. This point was notably examined in TMPTA and BisGMA/TEGDMA. Noticeably, the increase in the OH groups per dye adversely affected the solubility of dyes. Thus, the worse solubilities were determined for Chrysin and Myricetin.

Examination of their photoinitiating abilities during the FRP of TMPTA in thin films revealed the two-component dye/Iod3 system to be inefficient for promoting any polymerization. Conversely, by using the two-component dye/NPG system and the three-component dye/Iod3/NPG system, a monomer conversion could be detected with the different dyes. Among them, 6HF furnished good monomer conversions both at 385 and 405 nm. The highest monomer conversion was obtained at 385 nm, using the three-component 6HF/Iod3/NPG (0.5%/1%/1% *w*/*w*/*w*) system, resulting from the perfect adequation between the emission of the LED and the absorption of the chromophore. At 405 nm, a reduction in the monomer conversion by ca. 10% could be determined, consistent with a decrease in the molar extinction coefficient. Noticeably, an important effect of the additives could be evidenced. Thus, by using EDB as the amine in three-component systems, a severe reduction in the monomer conversion could be determined, compared to that obtained with NPG. This was assigned to the strong oxygen inhibition competing with initiation [52][96][97][98][99][100][101]. This point was evidenced by using 4-dppba as the additive. Indeed,

phosphines are well known to convert the unreactive peroxyl radicals as initiating alkoxyl radicals [97][102][103]. Using the three-component 6HF/Iod3/4-dppba (0.5%/1%/1% *w*/*w*/*w*) system at 385 nm, a conversion comparable to that obtained with the three-component 6HF/Iod3/NPG (0.5%/1%/1% *w*/*w*/*w*) system could be obtained.

The high reactivity of the three-component 6HF/Iod3/NPG (0.5%/1%/1% *w*/*w*/*w*) system was confirmed during the FRP experiments performed on another resin, i.e., a BisGMA/TEGDMA blend. Surprisingly, if 3-hydroxyflavone 3HF previously studied proved to be an efficient photoinitiator for promoting the CP of EPOX at 385 nm, only a low monomer conversion could be obtained with the two-component 6-hydroxyflavone/Iod3 (0.5%/1% *w*/*w*) (40% conversion after 800 s of irradiation at 385 nm vs. 55% for the three-component 3HF/Iod3/EDB (0.5%/1%/1% *w*/*w*/*w*)) system, evidencing the strong influence of the substitution pattern on the overall reactivity of the photoinitiating system. In addition, the high monomer conversion obtained during the FRP of BisGMA/TEGDMA paves the way for dental applications of flavones [104].

3. Proanthocyanidins

Proanthocyanidins are flavonoids that can be found in black, red and purple rice, in other strongly colored fruits and vegetables and also in cereals such as blueberries, grapes, red cabbages and purple sweet potatoes [105][106][107][108][109][110][111]. Due to their high molar extinction coefficients, proanthocyanidins were thus ideal candidates for photopolymerization performed under visible light. In 2021, Wang and coworkers examined a series of proanthocyanidins substituted with methacrylate groups (see **Figure 8**) [112][113].

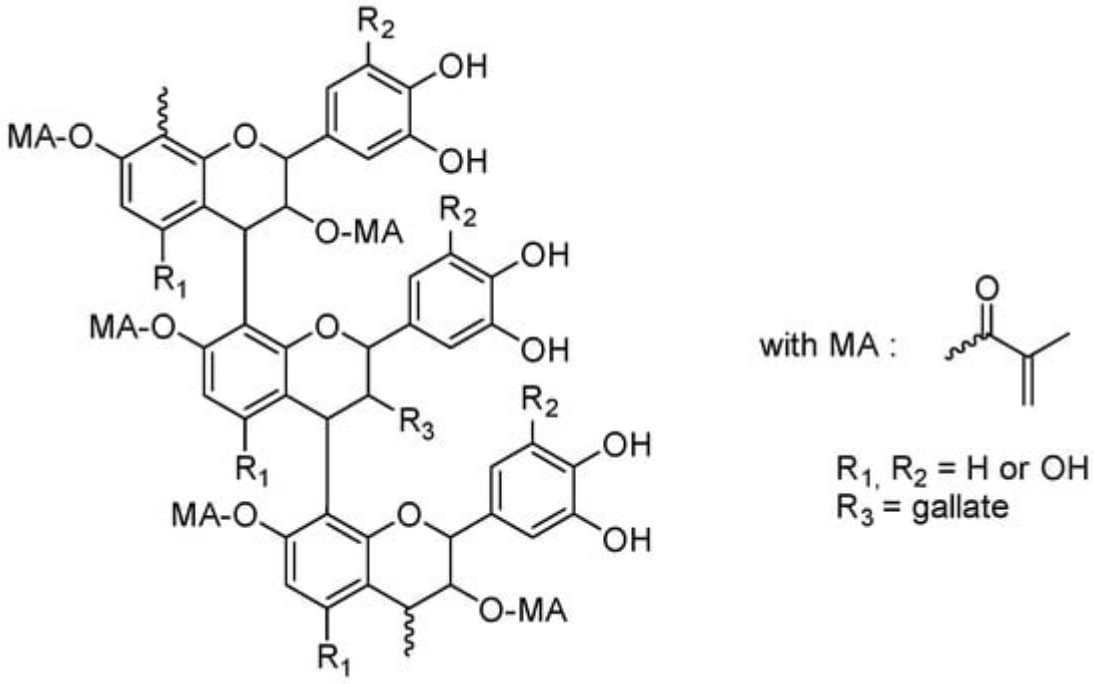

Figure 8. Chemical structures of methacrylate-based proanthocyanidins.

By the presence of methacrylate groups, polymerizable crosslinkers could be obtained, and the resulting polymers could be advantageously used for collagen stabilization in 2-hydroxyethylmethacrylate (HEMA)-based dental

adhesive systems. In particular, an improvement in the longevity of the dental restoration could be evidenced by using these modified proanthocyanins.

References

1. Rao, Y.J.; Sowjanya, T.; Thirupathi, G.; Murthy, N.Y.S.; Kotapalli, S.S. Synthesis and Biological Evaluation of Novel Flavone/Triazole/Benzimidazole Hybrids and Flavone/Isoxazole-Annulated Heterocycles as Antiproliferative and Antimycobacterial Agents. Mol. Divers. 2018, 22, 803–814.
2. Yu, H.; Kim, S.-H.; Lee, J.-Y.; Kim, H.-J.; Seo, S.-H.; Chung, B.-Y.; Jin, C.-B.; Lee, Y.-S. Synthesis and Antioxidant Activity of 3-Methoxyflavones. Bull. Korean Chem. Soc. 2005, 26, 2057–2060.
3. Balasuriya, N.; Rupasinghe, H.P.V. Antihypertensive Properties of Flavonoid-Rich Apple Peel Extract. Food Chem. 2012, 135, 2320–2325.
4. Li, J.-X.; Xue, B.; Chai, Q.; Liu, Z.-X.; Zhao, A.-P.; Chen, L.-B. Antihypertensive Effect of Total Flavonoid Fraction of Astragalus Complanatus in Hypertensive Rats. Chin. J. Physiol. 2005, 48, 101–106.
5. Kawai, M.; Hirano, T.; Higa, S.; Arimitsu, J.; Maruta, M.; Kuwahara, Y.; Ohkawara, T.; Hagihara, K.; Yamadori, T.; Shima, Y.; et al. Flavonoids and Related Compounds as Anti-Allergic Substances. Allergol. Int. 2007, 56, 113–123.
6. Orhan, D.D.; Özçelik, B.; Özgen, S.; Ergun, F. Antibacterial, Antifungal, and Antiviral Activities of Some Flavonoids. Microbiol. Res. 2010, 165, 496–504.
7. Inoue, T.; Sugimoto, Y.; Masuda, H.; Kamei, C. Antiallergic Effect of Flavonoid Glycosides Obtained from Mentha piperita L. Biol. Pharm. Bull. 2002, 25, 256–259.
8. Nijveldt, R.J.; van Nood, E.; van Hoorn, D.E.; Boelens, P.G.; van Norren, K.; van Leeuwen, P.A. Flavonoids: A Review of Probable Mechanisms of Action and Potential Applications123. Am. J. Clin. Nutr. 2001, 74, 418–425.
9. Forbes, A.M.; Lin, H.; Meadows, G.G.; Meier, G.P. Synthesis and Anticancer Activity of New Flavonoid Analogs and Inconsistencies in Assays Related to Proliferation and Viability Measurements. Int. J. Oncol. 2014, 45, 831–842.
10. Merzlyak, M.N.; Solovchenko, A.E.; Smagin, A.I.; Gitelson, A.A. Apple Flavonols during Fruit Adaptation to Solar Radiation: Spectral Features and Technique for Non-Destructive Assessment. J. Plant Physiol. 2005, 162, 151–160.
11. Tamer, Ö.; Şimşek, M.; Avcı, D.; Atalay, Y. First and Second Order Hyperpolarizabilities of Flavonol Derivatives: A Density Functional Theory Study. Spectrochim. Acta Part A Mol. Biomol. Spectrosc. 2022, 283, 121728.

12. Yuan, H.; Jiang, A.; Fang, H.; Chen, Y.; Guo, Z. Optical Properties of Natural Small Molecules and Their Applications in Imaging and Nanomedicine. Adv. Drug Deliv. Rev. 2021, 179, 113917.
13. Yang, Q.; Muchová, L.; Štacková, L.; Štacko, P.; Šindelář, V.; Vítek, L.; Klán, P. Cyanine–Flavonol Hybrids as NIR-Light Activatable Carbon Monoxide Donors in Methanol and Aqueous Solutions. Chem. Commun. 2022, 58, 8958–8961.
14. Höfener, S.; Kooijman, P.C.; Groen, J.; Ariese, F.; Visscher, L. Fluorescence Behavior of (Selected) Flavonols: A Combined Experimental and Computational Study. Phys. Chem. Chem. Phys. 2013, 15, 12572–12581.
15. Sengupta, P.K.; Kasha, M. Excited State Proton-Transfer Spectroscopy of 3-Hydroxyflavone and Quercetin. Chem. Phys. Lett. 1979, 68, 382–385.
16. Strandjord, A.J.G.; Courtney, S.H.; Friedrich, D.M.; Barbara, P.F. Excited-State Dynamics of 3-Hydroxyflavone. J. Phys. Chem. 1983, 87, 1125–1133.
17. McMorrow, D.; Kasha, M. Intramolecular Excited-State Proton Transfer in 3-Hydroxyflavone. Hydrogen-Bonding Solvent Perturbations. J. Phys. Chem. 1984, 88, 2235–2243.
18. Schwartz, B.J.; Peteanu, L.A.; Harris, C.B. Direct Observation of Fast Proton Transfer: Femtosecond Photophysics of 3-Hydroxyflavone. J. Phys. Chem. 1992, 96, 3591–3598.
19. Ameer-Beg, S.; Ormson, S.M.; Brown, R.G.; Matousek, P.; Towrie, M.; Nibbering, E.T.J.; Foggi, P.; Neuwahl, F.V.R. Ultrafast Measurements of Excited State Intramolecular Proton Transfer (ESIPT) in Room Temperature Solutions of 3-Hydroxyflavone and Derivatives. J. Phys. Chem. A 2001, 105, 3709–3718.
20. Roshal, A.D.; Grigorovich, A.V.; Doroshenko, A.O.; Pivovarenko, V.G.; Demchenko, A.P. Flavonols as Metal-Ion Chelators: Complex Formation with Mg2+ and Ba2+ Cations in the Excited State. J. Photochem. Photobiol. A Chem. 1999, 127, 89–100.
21. Smith, G.J.; Markham, K.R. Tautomerism of Flavonol Glucosides: Relevance to Plant UV Protection and Flower Colour. J. Photochem. Photobiol. A Chem. 1998, 118, 99–105.
22. Feng, W.; Wang, Y.; Chen, S.; Wang, C.; Wang, S.; Li, S.; Li, H.; Zhou, G.; Zhang, J. 4-Nitroimidazole-3-Hydroxyflavone Conjugate as a Fluorescent Probe for Hypoxic Cells. Dye. Pigment. 2016, 131, 145–153.
23. Dyrager, C.; Friberg, A.; Dahlén, K.; Fridén-Saxin, M.; Börjesson, K.; Wilhelmsson, L.M.; Smedh, M.; Grøtli, M.; Luthman, K. 2,6,8-Trisubstituted 3-Hydroxychromone Derivatives as Fluorophores for Live-Cell Imaging. Chem.–Eur. J. 2009, 15, 9417–9423.
24. Chen, S.; Hou, P.; Zhou, B.; Song, X.; Wu, J.; Zhang, H.; Foley, J.W. A Red Fluorescent Probe for Thiols Based on 3-Hydroxyflavone and Its Application in Living Cell Imaging. RSC Adv. 2013, 3, 11543–11546.

25. Liu, B.; Luo, Z.; Si, S.; Zhou, X.; Pan, C.; Wang, L. A Photostable Triphenylamine-Based Flavonoid Dye: Solvatochromism, Aggregation-Induced Emission Enhancement, Fabrication of Organic Nanodots, and Cell Imaging Applications. Dye. Pigment. 2017, 142, 32–38.
26. Dong, L.-Y.; Wang, L.-Y.; Wang, X.-F.; Liu, Y.; Liu, H.-L.; Xie, M.-X. Development of Fluorescent FRET Probe for Determination of Glucose Based on β-Cyclodextrin Modified ZnS-Quantum Dots and Natural Pigment 3-Hydroxyflavone. Dye. Pigment. 2016, 128, 170–178.
27. Tomin, V.I.; Ushakou, D.V. Use of 3-Hydroxyflavone as a Fluorescence Probe for the Controlled Photopolymerization of the E-Shell 300 Polymer. Polym. Test. 2017, 64, 77–82.
28. Woolfe, G.J.; Thistlethwaite, P.J. Direct Observation of Excited State Intramolecular Proton Transfer Kinetics in 3-Hydroxyflavone. J. Am. Chem. Soc. 1981, 103, 6916–6923.
29. Itoh, M.; Tokumura, K.; Tanimoto, Y.; Okada, Y.; Takeuchi, H.; Obi, K.; Tanaka, I. Time-Resolved and Steady-State Fluorescence Studies of the Excited-State Proton Transfer in 3-Hydroxyflavone and 3-Hydroxychromone. J. Am. Chem. Soc. 1982, 104, 4146–4150.
30. Itoh, M.; Fujiwara, Y. Two-Step Laser Excitation Fluorescence Study of the Ground- and Excited-State Proton Transfer in 3-Hydroxyflavone and 3-Hydroxychromone. J. Phys. Chem. 1983, 87, 4558–4560.
31. Ernsting, N.P.; Dick, B. Fluorescence Excitation of Isolated, Jet-Cooled 3-Hydroxyflavone: The Rate of Excited State Intramolecular Proton Transfer from Homogeneous Linewidths. Chem. Phys. 1989, 136, 181–186.
32. Sarkar, M.; Sengupta, P.K. Influence of Different Micellar Environments on the Excited-State Proton-Transfer Luminescence of 3-Hydroxyflavone. Chem. Phys. Lett. 1991, 179, 68–72.
33. Dick, B. AM1 and INDO/S Calculations on Electronic Singlet and Triplet States Involved in Excited-State Intramolecular Proton Transfer of 3-Hydroxyflavone. J. Phys. Chem. 1990, 94, 5752–5756.
34. Ramešová, Š.; Sokolová, R.; Degano, I. The Study of the Oxidation of the Natural Flavonol Fisetin Confirmed Quercetin Oxidation Mechanism. Electrochim. Acta 2015, 182, 544–549.
35. Pietta, P.-G. Flavonoids as Antioxidants. J. Nat. Prod. 2000, 63, 1035–1042.
36. Agati, G.; Azzarello, E.; Pollastri, S.; Tattini, M. Flavonoids as Antioxidants in Plants: Location and Functional Significance. Plant Sci. 2012, 196, 67–76.
37. Martinez, M.L.; Studer, S.L.; Chou, P.T. Direct Evidence of the Triplet-State Origin of the Slow Reverse Proton Transfer Reaction of 3-Hydroxyflavone. J. Am. Chem. Soc. 1990, 112, 2427–2429.
38. Yokoe, I.; Higuchi, K.; Shirataki, Y.; Komatsu, M. Photochemistry of Flavonoids. III. Photorearrangement of Flavonols. Chem. Pharm. Bull. 1981, 29, 894–898.

39. Matsuura, T.; Takemoto, T.; Nakashima, R. Photoinduced Reactions—LXXI: Photorearrangement of 3-Hydroxyflavones to 3-Aryl-3-Hydroxy-1,2-Indandiones. Tetrahedron 1973, 29, 3337–3340.
40. Tehfe, M.-A.; Dumur, F.; Xiao, P.; Graff, B.; Morlet-Savary, F.; Fouassier, J.-P.; Gigmes, D.; Lalevée, J. New Chromone Based Photoinitiators for Polymerization Reactions under Visible Light. Polym. Chem. 2013, 4, 4234–4244.
41. Tehfe, M.-A.; Dumur, F.; Telitel, S.; Gigmes, D.; Contal, E.; Bertin, D.; Morlet-Savary, F.; Graff, B.; Fouassier, J.-P.; Lalevée, J. Zinc-Based Metal Complexes as New Photocatalysts in Polymerization Initiating Systems. Eur. Polym. J. 2013, 49, 1040–1049.
42. Tehfe, M.-A.; Lalevée, J.; Morlet-Savary, F.; Graff, B.; Blanchard, N.; Fouassier, J.-P. Tunable Organophotocatalysts for Polymerization Reactions Under Visible Lights. Macromolecules 2012, 45, 1746–1752.
43. Lalevée, J.; Tehfe, M.-A.; Zein-Fakih, A.; Ball, B.; Telitel, S.; Morlet-Savary, F.; Graff, B.; Fouassier, J.P. N-Vinylcarbazole: An Additive for Free Radical Promoted Cationic Polymerization upon Visible Light. ACS Macro Lett. 2012, 1, 802–806.
44. Condat, M.; Babinot, J.; Tomane, S.; Malval, J.-P.; Kang, I.-K.; Spillebout, F.; Mazeran, P.-E.; Lalevée, J.; Andalloussi, S.A.; Versace, D.-L. Development of Photoactivable Glycerol-Based Coatings Containing Quercetin for Antibacterial Applications. RSC Adv. 2016, 6, 18235–18245.
45. Niedre, M.J.; Secord, A.J.; Patterson, M.S.; Wilson, B.C. In Vitro Tests of the Validity of Singlet Oxygen Luminescence Measurements as a Dose Metric in Photodynamic Therapy. Cancer Res. 2003, 63, 7986–7994.
46. Ragàs, X.; Cooper, L.P.; White, J.H.; Nonell, S.; Flors, C. Quantification of Photosensitized Singlet Oxygen Production by a Fluorescent Protein. ChemPhysChem 2011, 12, 161–165.
47. Ragàs, X.; Agut, M.; Nonell, S. Singlet Oxygen in Escherichia Coli: New Insights for Antimicrobial Photodynamic Therapy. Free Radic. Biol. Med. 2010, 49, 770–776.
48. Cahan, R.; Schwartz, R.; Langzam, Y.; Nitzan, Y. Light-Activated Antibacterial Surfaces Comprise Photosensitizers. Photochem. Photobiol. 2011, 87, 1379–1386.
49. Oh, K.W.; Choi, H.-M.; Kim, J.M.; Park, J.H.; Park, I.S. A Novel Antimicrobial Photosensitizer: Hydroxyethyl Michler’s Ketone. Text. Res. J. 2014, 84, 808–818.
50. Freire, F.; Costa, A.C.B.P.; Pereira, C.A.; Beltrame Junior, M.; Junqueira, J.C.; Jorge, A.O.C. Comparison of the Effect of Rose Bengal- and Eosin Y-Mediated Photodynamic Inactivation on Planktonic Cells and Biofilms of Candida Albicans. Lasers Med. Sci. 2014, 29, 949–955.
51. Guo, Y.; Rogelj, S.; Zhang, P. Rose Bengal-Decorated Silica Nanoparticles as Photosensitizers for Inactivation of Gram-Positive Bacteria. Nanotechnology 2010, 21, 065102.

52. Felgenträger, A.; Maisch, T.; Späth, A.; Schröder, J.A.; Bäumler, W. Singlet Oxygen Generation in Porphyrin-Doped Polymeric Surface Coating Enables Antimicrobial Effects on Staphylococcus Aureus. Phys. Chem. Chem. Phys. 2014, 16, 20598–20607.
53. Yano, S.; Hirohara, S.; Obata, M.; Hagiya, Y.; Ogura, S.; Ikeda, A.; Kataoka, H.; Tanaka, M.; Joh, T. Current States and Future Views in Photodynamic Therapy. J. Photochem. Photobiol. C Photochem. Rev. 2011, 12, 46–67.
54. Cohn, G.E.; Tseng, H.Y. Photodynamic Inactivation of Yeast Sensitized by Eosin Y. Photochem. Photobiol. 1977, 26, 465–474.
55. Usacheva, M.N.; Teichert, M.C.; Biel, M.A. Comparison of the Methylene Blue and Toluidine Blue Photobactericidal Efficacy against Gram-Positive and Gram-Negative Microorganisms. Lasers Surg. Med. 2001, 29, 165–173.
56. Bovis, M.J.; Noimark, S.; Woodhams, J.H.; Kay, C.W.M.; Weiner, J.; Peveler, W.J.; Correia, A.; Wilson, M.; Allan, E.; Parkin, I.P.; et al. Photosensitisation Studies of Silicone Polymer Doped with Methylene Blue and Nanogold for Antimicrobial Applications. RSC Adv. 2015, 5, 54830–54842.
57. Araújo, P.V.; Teixeira, K.I.R.; Lanza, L.D.; Cortes, M.E.; Poletto, L.T.A. In Vitro Lethal Photosensitization of S. Mutans Using Methylene Blue and Toluidine Blue o as Photosensitizers. Acta Odontológica Latinoam. 2009, 22, 93–97.
58. Brown, J.P. A Review of the Genetic Effects of Naturally Occurring Flavonoids, Anthraquinones and Related Compounds. Mutat. Res./Rev. Genet. Toxicol. 1980, 75, 243–277.
59. Read, M.A. Flavonoids: Naturally Occurring Anti-Inflammatory Agents. Am. J. Pathol. 1995, 147, 235–237.
60. Ohnishi, E.; Bannai, H. Quercetin Potentiates TNF-Induced Antiviral Activity. Antivir. Res. 1993, 22, 327–331.
61. Zhu, D.; Peng, X.; Xiao, P. Penta-Hydroxy Flavones-Based Photoinitiating Systems for Free Radical, Cationic, and Thiol-Ene Polymerization upon Exposure to Mild Blue LEDs. Macromol. Mater. Eng. 2021, 306, 2100059.
62. Lee, J.; Jin, H.; Lee, W.S.; Nagappan, A.; Choi, Y.H.; Kim, G.S.; Jung, J.; Ryu, C.H.; Shin, S.C.; Hong, S.C.; et al. Morin, a Flavonoid from Moraceae, Inhibits Cancer Cell Adhesion to Endothelial Cells and EMT by Downregulating VCAM1 and Ncadherin. Asian Pac. J. Cancer Prev. 2016, 17, 3071–3075.
63. Lee, Y.J.; Kim, W.I.; Kim, S.Y.; Cho, S.W.; Nam, H.S.; Lee, S.H.; Cho, M.K. Flavonoid Morin Inhibits Proliferation and Induces Apoptosis of Melanoma Cells by Regulating Reactive Oxygen Species, Sp1 and Mcl-1. Arch. Pharmacal Res. 2019, 42, 531–542.

64. Rajput, S.A.; Wang, X.; Yan, H.-C. Morin Hydrate: A Comprehensive Review on Novel Natural Dietary Bioactive Compound with Versatile Biological and Pharmacological Potential. Biomed. Pharmacother. 2021, 138, 111511.
65. Olayinka, E.T.; Ore, A.; Adeyemo, O.A.; Ola, O.S. The Role of Flavonoid Antioxidant, Morin in Improving Procarbazine-Induced Oxidative Stress on Testicular Function in Rat. Porto Biomed. J. 2019, 4, e28.
66. Matsumoto, A. Polymerization of Multiallyl Monomers. Prog. Polym. Sci. 2001, 26, 189–257.
67. Hoyle, C.E.; Lee, T.Y.; Roper, T. Thiol–Enes: Chemistry of the Past with Promise for the Future. J. Polym. Sci. Part A Polym. Chem. 2004, 42, 5301–5338.
68. Hata, E.; Mitsube, K.; Momose, K.; Tomita, Y. Holographic Nanoparticle-Polymer Composites Based on Step-Growth Thiol-Ene Photopolymerization. Opt. Mater. Express 2011, 1, 207–222.
69. Al Mousawi, A.; Garra, P.; Schmitt, M.; Toufaily, J.; Hamieh, T.; Graff, B.; Fouassier, J.P.; Dumur, F.; Lalevée, J. 3-Hydroxyflavone and N-Phenylglycine in High Performance Photoinitiating Systems for 3D Printing and Photocomposites Synthesis. Macromolecules 2018, 51, 4633–4641.
70. Garra, P.; Graff, B.; Morlet-Savary, F.; Dietlin, C.; Becht, J.-M.; Fouassier, J.-P.; Lalevée, J. Charge Transfer Complexes as Pan-Scaled Photoinitiating Systems: From 50 Mm 3D Printed Polymers at 405 Nm to Extremely Deep Photopolymerization (31 Cm). Macromolecules 2018, 51, 57–70.
71. Bonifačić, M.; Štefanić, I.; Hug, G.L.; Armstrong, D.A.; Asmus, K.-D. Glycine Decarboxylation: The Free Radical Mechanism. J. Am. Chem. Soc. 1998, 120, 9930–9940.
72. Ullrich, G.; Burtscher, P.; Salz, U.; Moszner, N.; Liska, R. Phenylglycine Derivatives as Coinitiators for the Radical Photopolymerization of Acidic Aqueous Formulations. J. Polym. Sci. Part A Polym. Chem. 2006, 44, 115–125.
73. You, J.; Fu, H.; Zhao, D.; Hu, T.; Nie, J.; Wang, T. Flavonol Dyes with Different Substituents in Photopolymerization. J. Photochem. Photobiol. A Chem. 2020, 386, 112097.
74. You, J.; Cao, D.; Hu, T.; Ye, Y.; Jia, X.; Li, H.; Hu, X.; Dong, Y.; Ma, Y.; Wang, T. Novel Norrish Type I Flavonoid Photoinitiator for Safe LED Light with High Activity and Low Toxicity by Inhibiting the ESIPT Process. Dye. Pigment. 2021, 184, 108865.
75. You, J.; Du, Y.; Xue, T.; Bao, B.; Hu, T.; Ye, Y.; Wang, T. The Three-Component Photoinitiating Systems Based on Flavonol Sulfonate and Application in 3D Printing. Dye. Pigment. 2022, 197, 109899.
76. Chen, H.; Noirbent, G.; Zhang, Y.; Sun, K.; Liu, S.; Brunel, D.; Gigmes, D.; Graff, B.; Morlet-Savary, F.; Xiao, P.; et al. Photopolymerization and 3D/4D Applications Using Newly Developed

Dyes: Search around the Natural Chalcone Scaffold in Photoinitiating Systems. Dye. Pigment. 2021, 188, 109213.

77. Chen, H.; Noirbent, G.; Liu, S.; Brunel, D.; Graff, B.; Gigmes, D.; Zhang, Y.; Sun, K.; Morlet-Savary, F.; Xiao, P.; et al. Bis-Chalcone Derivatives Derived from Natural Products as near-UV/Visible Light Sensitive Photoinitiators for 3D/4D Printing. Mater. Chem. Front. 2021, 5, 901–916.
78. Chen, H.; Regeard, C.; Salmi, H.; Morlet-Savary, F.; Giacoletto, N.; Nechab, M.; Xiao, P.; Dumur, F.; Lalevée, J. Interpenetrating Polymer Network Hydrogels Using Natural Based Dyes Initiating Systems: Antibacterial Activity and 3D/4D Performance. Eur. Polym. J. 2022, 166, 111042.
79. Chen, H.; Noirbent, G.; Zhang, Y.; Brunel, D.; Gigmes, D.; Morlet-Savary, F.; Graff, B.; Xiao, P.; Dumur, F.; Lalevée, J. Novel D–π-A and A–π-D–π-A Three-Component Photoinitiating Systems Based on Carbazole/Triphenylamino Based Chalcones and Application in 3D and 4D Printing. Polym. Chem. 2020, 11, 6512–6528.
80. Li, M.; Du, Y.; Zhan, H.; Zhang, L.; Wu, H.; Zhao, D.; Wang, Q.; Wang, T. Synthesis and Photochemistry of Flavonol Camphorsulfonates Photoinitiator with Different Substituents. Prog. Org. Coat. 2023, 183, 107810.
81. Brahmachari, G.; Nurjamal, K.; Karmakar, I.; Mandal, M. Camphor-10-Sulfonic Acid (CSA): A Water Compatible Organocatalyst in Organic Transformations. Curr. Organocatal. 2018, 5, 165–181.
82. Fehr, M.; Appl, Á.; Esdaile, D.J.; Naumann, S.; Schulz, M.; Dahms, I. D-10-Camphorsulfonic Acid: Safety Evaluation. Mutat. Res./Genet. Toxicol. Environ. Mutagen. 2020, 858–860, 503257.
83. Andraos, J.; Barclay, G.G.; Medeiros, D.R.; Baldovi, M.V.; Scaiano, J.C.; Sinta, R. Model Studies on the Photochemistry of Phenolic Sulfonate Photoacid Generators. Chem. Mater. 1998, 10, 1694–1699.
84. He, B.-H.; He, J.; Wang, G.-X.; Liu, L.-C.; Wu, H.; Zhong, M. Photoinduced Controlled/“Living” Polymerization of Methyl Methacrylate with Flavone as Photoinitiator. J. Appl. Polym. Sci. 2016, 133, 43845.
85. Al Mousawi, A.; Garra, P.; Dumur, F.; Graff, B.; Fouassier, J.P.; Lalevée, J. Flavones as Natural Photoinitiators for Light Mediated Free-Radical Polymerization via Light Emitting Diodes. J. Polym. Sci. 2020, 58, 254–262.
86. Miean, K.H.; Mohamed, S. Flavonoid (Myricetin, Quercetin, Kaempferol, Luteolin, and Apigenin) Content of Edible Tropical Plants. J. Agric. Food Chem. 2001, 49, 3106–3112.
87. Walle, T.; Otake, Y.; Brubaker, J.A.; Walle, U.K.; Halushka, P.V. Disposition and Metabolism of the Flavonoid Chrysin in Normal Volunteers. Br. J. Clin. Pharmacol. 2001, 51, 143–146.

88. Jana, K.; Yin, X.; Schiffer, R.B.; Chen, J.-J.; Pandey, A.K.; Stocco, D.M.; Grammas, P.; Wang, X. Chrysin, a Natural Flavonoid Enhances Steroidogenesis and Steroidogenic Acute Regulatory Protein Gene Expression in Mouse Leydig Cells. J. Endocrinol. 2008, 197, 315–323.

89. Oliveira, G.A.R.; Ferraz, E.R.A.; Souza, A.O.; Lourenço, R.A.; Oliveira, D.P.; Dorta, D.J. Evaluation of the Mutagenic Activity of Chrysin, a Flavonoid Inhibitor of the Aromatization Process. J. Toxicol. Environ. Health Part A 2012, 75, 1000–1011.

90. Manzolli, E.S.; Serpeloni, J.M.; Grotto, D.; Bastos, J.K.; Antunes, L.M.G.; Barbosa, F.; Barcelos, G.R.M. Protective Effects of the Flavonoid Chrysin against Methylmercury-Induced Genotoxicity and Alterations of Antioxidant Status, In Vivo. Oxidative Med. Cell. Longev. 2015, 2015, 602360.

91. Flores-Aguilar, L.Á.; Cueto-Escobedo, J.; Puga-Olguín, A.; Olmos-Vázquez, O.J.; Rosas-Sánchez, G.U.; Bernal-Morales, B.; Rodríguez-Landa, J.F. Behavioral Despair Is Blocked by the Flavonoid Chrysin (5,7-Dihydroxyflavone) in a Rat Model of Surgical Menopause. Molecules 2023, 28, 587.

92. Lin, C.C.; Yu, C.S.; Yang, J.S.; Lu, C.C.; Chiang, J.H.; Lin, J.P.; Kuo, C.-L.; Chung, J.G. Chrysin, a Natural and Biologically Active Flavonoid, Influences a Murine Leukemia Model In Vivo through Enhancing Populations of T-and B-Cells, and Promoting Macrophage Phagocytosis and NK Cell Cytotoxicity. In Vivo 2012, 26, 665.

93. Mohos, V.; Fliszár-Nyúl, E.; Ungvári, O.; Bakos, É.; Kuffa, K.; Bencsik, T.; Zsidó, B.Z.; Hetényi, C.; Telbisz, Á.; Özvegy-Laczka, C.; et al. Effects of Chrysin and Its Major Conjugated Metabolites Chrysin-7-Sulfate and Chrysin-7-Glucuronide on Cytochrome P450 Enzymes and on OATP, P-Gp, BCRP, and MRP2 Transporters. Drug Metab Dispos 2020, 48, 1064.

94. Huang, J.; Yves Le Gac, P.; Richaud, E. Thermal Oxidation of Poly(Dicyclopentadiene)-Effect of Phenolic and Hindered Amine Stabilizers. Polym. Degrad. Stab. 2021, 183, 109267.

95. Pavlinec, J.; Kleinová, A.; Moszner, N. The Depletion of Substituted Phenolic Stabilizers by Conjugate C-Addition to Acrylic Monomers in Multicomponent Systems. Macromol. Mater. Eng. 2012, 297, 1005–1013.

96. Belon, C.; Allonas, X.; Croutxé-barghorn, C.; Lalevée, J. Overcoming the Oxygen Inhibition in the Photopolymerization of Acrylates: A Study of the Beneficial Effect of Triphenylphosphine. J. Polym. Sci. Part A Polym. Chem. 2010, 48, 2462–2469.

97. Bouzrati-Zerelli, M.; Maier, M.; Fik, C.P.; Dietlin, C.; Morlet-Savary, F.; Fouassier, J.P.; Klee, J.E.; Lalevée, J. A Low Migration Phosphine to Overcome the Oxygen Inhibition in New High Performance Photoinitiating Systems for Photocurable Dental Type Resins. Polym. Int. 2017, 66, 504–511.

98. Courtecuisse, F.; Belbakra, A.; Croutxé-Barghorn, C.; Allonas, X.; Dietlin, C. Zirconium Complexes to Overcome Oxygen Inhibition in Free-Radical Photopolymerization of Acrylates: Kinetic,

Mechanism, and Depth Profiling. J. Polym. Sci. Part A Polym. Chem. 2011, 49, 5169–5175.

99. Xu, F.; Yang, J.-L.; Gong, Y.-S.; Ma, G.-P.; Nie, J. A Fluorinated Photoinitiator for Surface Oxygen Inhibition Resistance. Macromolecules 2012, 45, 1158–1164.
100. Yang, Q.; Lalevée, J.; Poly, J. Development of a Robust Photocatalyzed ATRP Mechanism Exhibiting Good Tolerance to Oxygen and Inhibitors. Macromolecules 2016, 49, 7653–7666.
101. Yeow, J.; Shanmugam, S.; Corrigan, N.; Kuchel, R.P.; Xu, J.; Boyer, C. A Polymerization-Induced Self-Assembly Approach to Nanoparticles Loaded with Singlet Oxygen Generators. Macromolecules 2016, 49, 7277–7285.
102. Kirschner, J.; Becht, J.-M.; Klee, J.E.; Lalevée, J. A New Phosphine for Efficient Free Radical Polymerization under Air. Macromol. Rapid Commun. 2020, 41, 2000053.
103. Dietlin, C.; Trinh, T.T.; Schweizer, S.; Graff, B.; Morlet-Savary, F.; Noirot, P.-A.; Lalevée, J. New Phosphine Oxides as High Performance Near- UV Type I Photoinitiators of Radical Polymerization. Molecules 2020, 25, 1671.
104. Abdul-Monem, M.M. Naturally Derived Photoinitiators for Dental and Biomaterials Applications. Eur. Dent. Res. Biomater. J. 2021, 1, 72–78.
105. Limtrakul, P.; Semmarath, W.; Mapoung, S. Anthocyanins and Proanthocyanidins in Natural Pigmented Rice and Their Bioactivities. In Phytochemicals in Human Health; Rao, V., Mans, D., Rao, L., Eds.; IntechOpen: Rijeka, Croatia, 2019; Chapter 1; ISBN 978-1-78985-588-3.
106. Mannino, G.; Chinigò, G.; Serio, G.; Genova, T.; Gentile, C.; Munaron, L.; Bertea, C.M. Proanthocyanidins and Where to Find Them: A Meta-Analytic Approach to Investigate Their Chemistry, Biosynthesis, Distribution, and Effect on Human Health. Antioxidants 2021, 10, 1229.
107. Rauf, A.; Imran, M.; Abu-Izneid, T.; Iahtisham-Ul-Haq; Patel, S.; Pan, X.; Naz, S.; Sanches Silva, A.; Saeed, F.; Rasul Suleria, H.A. Proanthocyanidins: A Comprehensive Review. Biomed. Pharmacother. 2019, 116, 108999.
108. Nie, Y.; Stürzenbaum, S.R. Proanthocyanidins of Natural Origin: Molecular Mechanisms and Implications for Lipid Disorder and Aging-Associated Diseases. Adv. Nutr. 2019, 10, 464–478.
109. Nie, F.; Liu, L.; Cui, J.; Zhao, Y.; Zhang, D.; Zhou, D.; Wu, J.; Li, B.; Wang, T.; Li, M.; et al. Oligomeric Proanthocyanidins: An Updated Review of Their Natural Sources, Synthesis, and Potentials. Antioxidants 2023, 12, 1004.
110. Dixon, R.A.; Xie, D.-Y.; Sharma, S.B. Proanthocyanidins–a Final Frontier in Flavonoid Research? New Phytol. 2005, 165, 9–28.
111. Yang, K.; Chan, C.B. Proposed Mechanisms of the Effects of Proanthocyanidins on Glucose Homeostasis. Nutr. Rev. 2017, 75, 642–657.

112. Hass, V.; Li, Y.; Wang, R.; Nguyen, D.; Peng, Z.; Wang, Y. Methacrylate-Functionalized Proanthocyanidins as Novel Polymerizable Collagen Cross-Linkers–Part 1: Efficacy in Dentin Collagen Bio-Stabilization and Cross-Linking. Dent. Mater. 2021, 37, 1183–1192.

113. Wang, R.; Li, Y.; Hass, V.; Peng, Z.; Wang, Y. Methacrylate-Functionalized Proanthocyanidins as Novel Polymerizable Collagen Cross-Linkers—Part 2: Effects on Polymerization, Microhardness and Leaching of Adhesives. Dent. Mater. 2021, 37, 1193–1201.